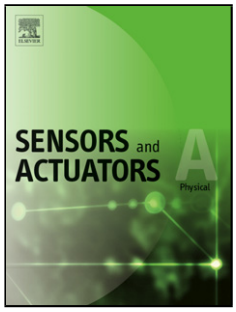

Title: Electrical Impedance Performance of Metal Dry Bioelectrode with Different Surface Coatings

Authors: Wei Liu, Wei Zhou, Shaoyu Liu, Chenying Zhang, Shuaishuai Huang, Yaoyao Li, Kwan San Hui

PII: S0924-4247(17)31675-8
DOI: https://doi.org/10.1016/j.sna.2017.12.006
Reference: SNA 10493

To appear in: *Sensors and Actuators A*

Received date: 17-9-2017
Revised date: 29-11-2017
Accepted date: 4-12-2017

Please cite this article as: Liu W, Zhou W, Liu S, Zhang C, Huang S, Li Y, Hui KS, Electrical Impedance Performance of Metal Dry Bioelectrode with Different Surface Coatings, *Sensors and Actuators: A Physical* (2010), https://doi.org/10.1016/j.sna.2017.12.006

Electrical Impedance Performance of Metal Dry Bioelectrode with Different Surface Coatings

Wei Liu [a], Wei Zhou [a *], Shaoyu Liu [a], Chenying Zhang [a], Shuaishuai Huang [a], Yaoyao Li [a], Kwan San Hui [b]

[a] *Department of Mechanical & Electrical Engineering, Xiamen University, Xiamen 361005, China*

[b] *School of Mathematics, Faculty of Science,University of East Anglia, Norwich, NR4 7TJ, United Kingdom*

*Corresponding author. Tel.: 86-592-2188698; Fax: 86-592-2186383

E-mail address: weizhou@xmu.edu.cn (Wei Zhou).

Highlights

> The metal dry bioelectrodes with different coating layers are developed. > Effect of coating layers on impedance performance of bioelectrode is studied. > Optimal electroplating time for silver layer of bioelectrode is 20 min. > The bioelectrode with Ag layer exhibits much lower impedance value. > Best impedance performance are obtained for bioelectrode with silver/silver chloride layer.

Abstract: To improve the electrical impedance performance of bioelectrodes, a novel metal dry bioelectrodes with different coating layers are developed with laser micromilling and electroplating technology. Based on the analysis of the coating layer on the bioelectrode surface, the effect of different coating layers on the electrical impedance performance of bioelectrodes is investigated. The results show that the

silver content increases with electroplating time when the silver layer is coated on the bioelectrode surface. However, the decrease of silver layer weight is observed with much longer electroplating time, and the optimal electroplating time is 20 min. Compared with the uncoated bioelectrode, the bioelectrode coated with silver layer exhibits much lower impedance value and better impedance stability. Especially, when the silver-coated bioelectrode is subsequently coated with silver-silver chloride layer, the lowest impedance value and best impedance stability are obtained.

Keywords: Dry bioelectrode; Laser micromilling; Electroplating technology; Silver layer; Silver/silver chloride layer

1 Introduction

Biomedical electrodes are extensively used in clinic diagnostics and therapeutic stimulation, including electrocardiographs (ECG), electroencephalograms (EEG), electromyography (EMG) and electrical impedance tomography (EIT) [1-4]. Since the bioelectrical signal belong to a kind of weak electrical signal, the design and fabrication of the bioelectrodes are a critical role for the measurement process of bioelectrical signal. Meanwhile, the interface properties between the bioelectrode and the skin also have drawn the attention of researchers from around the world. Generally, the lower contact impedance between bioelectrode and skin is desirable for measurement system. The higher contact impedance causes the larger attenuation of signal amplitude. Fortunately, the attenuation of signal amplitude could be

compensated with modern high input-impedance amplifiers. However, the signal distortion and interference phenomenon is easy to produce in the process [5-6]. To avoid these problems, many new types of bioelectrodes have been developed using different design and fabrication methods.

Wet electrodes, such as Ag/AgCl electrode, are widely applied to record the bioelectrical signal. The outer layer of human skin is composed several layers of dead cells, called the stratum corneum. The stratum corneum is electrically insulated and leads to produce the high contact impedance. In order to reduce the influence of stratum corneum , the wet electrodes need the processes of skin abrasion and a conductive gel. However, the skin abrasion is time-consuming and uncomfortable for the patients. Meanwhile, the conductive gel will dry up gradually and even cause swelling and allergy in some cases [7-9]. These disadvantages make the wet electrodes difficult to accurately measure the bioelectrical signal in a long time. To solve these problems, some kinds of dry bioelectrodes are developed because the skin preparation and gel usage are not necessary. As in the earlier study, the metal plate dry electrode had a large noise and poor signal quality. These bioelectrodes could not conform to the irregular surface of skin during movement and the additional noise gets [10]. In recent years, there is a growing interest in the development of novel dry bioelectrodes, including foam backing dry bioelectrodes[11-13], fabric dry bioelectrodes [14] and microstructure dry bioelectrodes [15]. Among these bioelectrodes, the dry bioelectrodes with microstructure array show outstanding advantages of collect biosignal with less noise. The surface microstructure array of

bioelectrodes can increase the actual contact area between electrode and skin with the same geometrical dimension, resulting in the decrease of the contact impedance. In addition, the bioelectrodes with surface microstructure array can maintain good contact status with skin when a relative sliding occurs at the interface between electrode and skin, which contribute to a small motion artifact and a higher signal-to-noise ratio (SNR).

Up to now, many micro/nano fabrication technologies have been used to develop the dry bioelectrodes with surface microstructure array, including MEMS technology [16-18], vacuum casting technology [19], 3D printing technology [20], thermal drawing [21], micromolding [22] and magnetization-induced self-assembly [23]. The MEMS technology has been widely used to fabricate the spiked electrodes. Two different technologies such as deep dry etching combined with isotropic wet etching as well as mechanical dicing combined with chemical wet etching were selected to fabricate the microneedle arrays of dry electrode. And the 50/300 nanometer Ti/Au was sputtered on the microneedles and the backside of the wafers to measure the EEG signal [16]. Griss *et al* [17-18] fabricated silicon-based micromachined spiked electrodes by deep reactive ion etching method and were subsequently covered with a silver-silver chloride (Ag–AgCl) double layer. Ng *et al* [19] developed the micro-spike dry EEG electrodes by a vacuum casting method using a master pattern piece made by CNC micro-machining. A layer of conductive Ag coating was then deposited onto the surface of the dry micro-spike electrode by means of electroless plating. Salvo *et al* [20] proposed 3D printing method to fabricate the dry

bioelectrodes using the insulating acrylic photopolymer. The adhesion promotion layer of titanium (150 nm) and a gold layer (250 nm) was coated to reduce the impedance and prevent both corrosion and oxidation. Moreover, the thermal drawing method [21] and micromolding method [22] were also used to fabricate the polymer bioelectrodes with surface microstructured arrays. Recently, Jang *et al* [23] employed magnetization-induced self-assembly method to fabricate a microneedle array bioelectrode coated with Ti/Au film. Thus, the surface coatings is an important factor to improve the testing effectiveness when the bioelectrodes with microstructure array are used to measure the biopotential signal [24-25].

In this study, the laser micromilling technology was utilized to fabricate the dry bioelectrode with surface microstructure array. In order to reduce the contact impedance, the Ag layer and Ag–AgCl double layer were coated on the surface of bioelectrode by electroplating technology. The equivalent circuit model of electrode-skin interface was established to analyze the measured impedance of bioelectrode. Finally, the measured impedance of bioelectrodes with different surface coatings was compared to evaluate the electrical impedance performances.

2 Material and methods

2.1 Structural design of metal dry bioelectrode

The design of metal dry bioelectrode with surface microstructure array is shown in Fig.1. The metal dry bioelectrode consisted of a metal electrode core, a foam substrate, shielding wires, and conductive silver glue. The metal electrode core (Diameter=10 mm, Thickness=0.5 mm) was made of copper material (purity>99.9%).

In order to improve the contact status between bioelectrode and skin, the microstructure array was fabricated on the surface of bioelectrode core by laser micromilling. Both Ag layer and Ag–AgCl double layer were deposited on the surface of bioelectrode core to enhance the biological compatibility and protect the substrate material from oxidation. A foam substrate was attached to the smooth surface of bioelectrode core. The shape and the diameter of the foam backing were round and 15mm, respectively. The design of the foam backing could reduce the signal interference caused by the movement. The shielding wire penetrated into the foam backing and was connected to the smooth surface of bioelectrode core through conductive silver paste. Compared to other welding methods, the use of conductive silver glue could avoid the high impedance nodes.

2.2 Laser micromilling process of bioelectrode core

The surface microstructure array of bioelectrode core was fabricated by laser micromilling technology [26-28]. In the laser micromilling process, the heated metal liquid or gas is condensed and generate the metal recasting layer in the adjacent area. The metal recasting layer is usually undesirable which affects the flatness of the workpiece surface. Interestingly, by adjusting the laser processing parameters, the recasting layer was successfully utilized to produce the regular microstructural array on the surface of the bioelectrode core. In this study, a prototype pulsed fiber laser (IPG, No:YLP-1-100-20-20-CN, Germany) was used as the fabrication laser, as shown in Fig.2. The used laser was adjusted to produce 100ns pulse with central emission wavelength of 1064 nm at the repetition rate of 20 kHz. Laser output power

was set as 20 W while the number of scans was 20 times and the scanning speed was 500 mm/s. The specifications of characteristic parameters of the fiber laser system are given in Table 1. Following the laser micromilling process, the bioelectrode core was dipped in 1 mol/L hydrochloric acid (HCl) solution for 20s and was quickly dried up by air pump gun under high pressure. The surface morphology of the bioelectrode core was observed through a scanning electron microscope (SEM) (Hitachi SU70, Japan) and the material composition of surface coating of bioelectrodes were analyzed with energy-dispersive X-ray measurements (EDX).

2.3 Surface coating of bioelectrode

2.3.1 Coating of Ag layer

Electroplating technology was adopted to deposit the thin Ag layer on the surface microstructure array of bioelectrode because of its low cost and easy operation. In the electroplating process, the cyanide-free solution was selected to satisfy with requirement of environmental concerns [29]. Before electroplating, the bioelectrode was pre-treated and the bath was prepared. The bioelectrode core with surface microstructure array was cleaned in 10% (volume fraction) hot NaOH solution, and dipped in 1 mol/L HCl solution for 8-10s for surface activation [30]. The thiosulfate baths containing $AgNO_3$ main salt was conducted. Sodium hyposulfite ($Na_2S_2O_3$), silver nitrate ($AgNO_3$) and potassium metabisulfite ($K_2S_2O_5$) were dissolved in distilled water at 60 ℃. After pouring $K_2S_2O_5$ solution into $AgNO_3$ stirred solution, $Na_2S_2O_3$ solution was slowly added in the mixed solution and the yellowish clear solution was obtained. Later, some ammonium acetate (CH_3COONH_4) and

thiosemicarbazide (CH_5N_3S) were both dissolved in the yellowish clear solution. Finally, the distilled water was added to control the volume of the bath. The detailed parameters of the bath are shown in Table 2. The pH value of the bath was 5.83 which provided an acid environment [30]. The illustration of the electroplating process of bioelectrode is shown in Fig.3. A pure silver plate (5mm long, 5mm wide, 1mm thick, and mass fraction> 99.9%) acted as the anode and the pre-treated bioelectrode core acted as the cathode. The current density was controlled at 0.8 $A \cdot dm^{-2}$ [30]. The electroplating time lasted for 10 to 40 minutes while the temperature was about 25℃. After electroplating process, the coated bioelectrode core with thin Ag layer was cleaned by deionized water and dried up. The surface properties of the Ag coatings were measured by XPS (PHI Quantum 2000 ESCA Microprobe, USA). The XPS experiments were carried out at room temperature in an ultrahigh vacuum (UHV) system. The monochromated Al Kα1,2 (energy = 1486.60 eV) was used as the X-ray source.

2.3.2 Coating of Ag–AgCl double layer

The silver-coated bioelectrode core was chlorinated by electrochemical treatment, and the Ag–AgCl double layer was obtained on the surface microstructure array of bioelectrode [31]. To coat the Ag–AgCl double layer, the silver-coated electrode electroplated for 20 minutes in silver-containing bath acted as the anode. A pure silver plate (5 mm long, 5 mm wide, 0.5 mm thick, and mass fraction > 99.9%) was used as the cathode in the electroplating process. Both the anode and the cathode were soaked in the bath of 1 mol/L HCl solution (Xilong Chemical Co., Ltd., China). A voltage of

1.5V was applied to the electrodes in HCl solution for 5s [31-32]. After being cleaned by deionized water and dried up, the Ag–AgCl coated bioelectrode with microstructure array was obtained and could be used for bioelectrical measurement.

2.4 Electrode-skin impedance measurement

A two-electrode system was employed to measure the contact impedance between electrode and skin [33-34]. Before the tests, two dry bioelectrodes were put in the inner right forearm of human and the distance between them was 5 cm [34]. Both bioelectrodes were located in the middle of the arm, and the first one of the electrodes was 5 cm from the wrist. A cuff pressure meter was applied to sustain the stable pressure between electrode and skin. The contact impedance were measured by a high precision impedance analyzer (No: HIOKI Im3523, Japan) using 500 μA (rms) AC sinusoid signal and the current was provided to be safe to human [34]. The frequency range of the impedance analyzer was from 50Hz to 200 kHz. Short circuit and open circuit calibrations were carried out and the data measured in the initial 10 min was discarded to reduce system interference. The experiment under each parameter was repeated 5 times. Finally, the average value of the measured impedances was taken as the contact impedance and the standard deviation was taken as the error bar.

3 Results and discussion

3.1 Surface morphology of microstructure array of dry bioelectrode

The surface morphology of microstructure array of dry bioelectrode was shown in Fig.4. In previous study [35], we found that the stacking process of recast layer

could be controlled to form a microstructure array on the surface of the dry bioelectrode in the laser micromilling process. From these SEM results, the microstructure with truncated conical shape was easy to be observed. From the Fig.4, the tip diameter is about 60 μm and the peak-peak spacing between two adjacent microstructures is about 200 μm. When the scratch test was conducted using the SiC sandpaper with 2 kPa applied pressure, it was found that the surface microstructure array of dry bioelectrode exhibited good mechanical strength [36]. Comparing with other fabrication methods[16-18], this processing method can fabricate the microstructure array on the surface of the bioelectrode with low production cost and high efficiency.

3.2 Electroplating process of bioelectrodes

Fig.5 shows the Ag concentration on the surface of bioelectrodes after electroplating. It is found that the Ag concentration of bioelectrodes surface increased when the electroplating time ranged from 10 min to 20 min. When the electroplating time exceeded 20 min, the Ag concentration decreased with increasing electroplating time. Especially, when electroplating time was 20 min, the Ag concentration of bioelectrodes surface reached the maximum value of 88%, as shown in Fig.5a. In this status, the Ag layer can be considered to be covered with the bioelectrode surface. Furthermore, the X-ray photoelectron spectroscopy results indicated that the pure silver was coated on the surface of bioelectrodes, as shown in Fig.5.b. However, the Ag concentration was only 32% when the electroplating time was 40 min. At the beginning of the electroplating process, the silver ions near cathode in the plating

solution will obtain the electrons and be converted into silver solids. These silver solids were gradually deposited on the surface of bioelectrode. As the electroplating time increases, the Ag concentration on the bioelectrode surface was increased to produce a thicker Ag layer. Whereas, the bond strength between silver layer and the copper substrate was significantly affected by the thickness of silver layer. When the much thicker silver layer was coated on the surface of bioelectrodes, the bonding strength Ag layer was greatly decreased because of the copper growth stress in the electroplating process [37-38].

Fig.6 shows the measured impedance between electrode and skin when the electroplating time ranged from 10 min to 30 min. The measured impedance value was increased firstly and then decreased. Interestingly, when the electroplating time was 20 min, the measured impedance value exhibited the minimum value of 2150 Ω. Obviously, there was a good consistency between the measured impedance and Ag concentration and the better coated Ag layer produce the smaller measured impedance. This is because the better Ag layer was coated on surface of bioelectrode. At the same time, the electrical conductivity of silver is better than copper and the improvement of Ag concentration enhances the electrical conductivity of the bioelectrode. Thus, the electroplating time of 20 min is suggested to obtain the higher Ag concentration and produce the lower contact impedance for bioelectrode.

Later, to deposit the Ag–AgCl double layer on the surface of bioelectrode, the bioelectrode with silver coating was selected as anode with voltage input. In this way, the Ag as anode material will loses electrons and turns into silver ions, combining

with chlorine ions near the anode to produce silver chloride on the surface of bioelectrode. Moreover, the chloride element have been found on the surface of silver layer-coated bioelectrode. Therefore, it is indicated that the Ag–AgCl double layer have been obtained [31].

3.3 Impedance characterization of bioelectrodes

3.3.1 Equivalent circuit of electrode-skin model

The contact impedance (Z) between electrode and skin consists of the resistance caused by the charge storage in the interface and the capacitive reactance caused by the opposition to current through the electrode and the skin [39-40]. The measured impedance could be represented in Cartesian form:

$$Z = Z' + jZ'' \quad (1)$$

Where Z' represents the real part and Z'' represents the imaginary part. j represents the imaginary unit.

The measured impedance could also be represented in polar form:

$$Z = |Z|e^{j\theta} \quad (2)$$

Where is $|Z|$ the magnitude of the measured impedance, while θ is the phase of the measured impedance. θ could be expressed by this equation:

$$\theta = \tan^{-1}[Z''/Z'] \quad (3)$$

The model of electrode-skin interfaces could be based on an equivalent circuit that a charge transfer resistance (R_{ct}) and an interfacial constant phase element (CPE) in parallel and then in series with a resistance (R_s) due to the microstructure array of bioelectrode. The equivalent circuit is presented in Fig.8 and the equivalent impedance (Z_{eq}) is expressed by this equation:

$$Z_{eq} = R_s + (R_{ct} \parallel Z_{CPE}) \quad (4)$$

$$Z_{CPE} = 1/(T*(j*\omega)\wedge P) \quad (5)$$

Where R_s represents the total resistance of the test bioelectrodes, skin and the test cables, R_{ct} represents the faradaic charge transfer resistance between skin and bioelectrode, and Z_{CPE} represents the impedance of CPE. The CPE is used to take place capacitor to compensate for non-homogeneity in the system and is defined by CPE-T and CPE-P. T represents the value of CPE-T and P represents the value of CPE-P. ω represents the angular frequency of the AC signal and j represents the imaginary unit. The model could be calculated by a Z View software package [39-40].

3.3.2 Impedance characterization under different current frequencies

The measured impedance values of bioelectrode with different current frequencies are shown in Fig.9. From Fig.9a, it is found that the amplitude of measured impedance was decreased with increasing current frequency. At low frequencies, the amplitude of measured impedance of bioelectrode was changed greatly. The measured impedance amplitude of bioelectrode coated with Ag layer was decreased from 319 kΩ at 50 Hz to 11.6 kΩ at 6 kHz. For the bioelectrode coated with Ag–AgCl double layer, the measured impedance amplitude was decreased from 40.1 kΩ at 50 Hz to 3.18 kΩ at 6 kHz. The amplitude of measured impedance of bioelectrode presented a slightly change when the current frequency was larger than 50 kHz. At the same frequency, the amplitude of measured impedance of bioelectrode

coated with Ag–AgCl double layer was much lower than that of bioelectrode coated with Ag layer due to its good polarization property. The bioelectrode coated with Ag–AgCl double layer was mainly related to a resistive behaviour attributed to the ionic charge transfer and the electrode coated with Ag layer mainly involved capacitive coupling [41].

From Fig.9b, the phase shift of bioelectrode coated with Ag layer decreased from -59° at 50 Hz to -64° at 6 kHz. For bioelectrode coated with Ag–AgCl double layer, the phase shift decreased from -18° at 50 Hz to -67° at 6 kHz. The reason for the smaller phase shift of bioelectrode coated with Ag layer was that it proved to be polarized. In contrast, the bioelectrode coated with Ag–AgCl double layer demonstrated to be perfected non-polarized electrode and the phase shift was larger [42].

The equivalent circuit model for bioelectrode was set up and presented in Fig.8. Based on this model, both the measured value and the fitting results of impedance of bioelectrodes were presented in Fig.10. Although the nyquist curves of two bioelectrodes coated with Ag layer and Ag–AgCl double layer were significantly different, the measured value and the fitting values demonstrated the similar trend based on the proposed model. The model parameters of the two electrodes are shown in Table 3. From this table, the faradaic charge transfer resistance (R_{ct})of bioelectrode coated with Ag layer is far greater than that of bioelectrode coated with Ag–AgCl double layer. Generally, when current (i) flows through the electrode-skin interface, the faradaic charge transfer resistance results to an additional voltage (named

'over-potential' in electrochemical) equal to $i * R_{ct}$ .An ideal non-polarisable electrode would have no faradaic resistance and charge could be transferred across the skin-electrode interface leading to no voltage loss [43]. However, the real systems are all polarisable. The inert metal electrodes tend to be polarized electrode while bioelectrode coated with Ag–AgCl double layer is less polarized. Thus, much larger value of faradaic charge transfer resistance of electrode coated with Ag layer was obtained.

3.3.3 Impedance stability over time

Fig.11 show the measured impedances stability of two bioelectrodes coated with Ag layer and Ag–AgCl double layer. The measurement time of 10 min and the current frequency of 50 kHz were selected which was significant for medical measurements [44-46]. From Fig.11, two bioelectrodes coated with Ag layer and Ag–AgCl double layer demonstrated small impedance fluctuates. Within 10 min, for bioelectrode coated with Ag–AgCl double layer, the average impedance was 1187 Ω, the standard deviation of impedance was 16.8 Ω, and the ratio of standard deviation to mean value was 14.1%; for bioelectrode coated with Ag layer, the average impedance was 2362 Ω, the difference in impedance change is 34.7 Ω, and the ratio of standard deviation to mean value was 14.7%. Thus, the better impedance stability of bioelectrode coated with Ag–AgCl double layer was found comparing with the bioelectrode coated with Ag layer.

3.4 Impedance of bioelectrodes with different surface coatings

The amplitude of the measured impedance of bioelectrode with different surface

coatings was shown in Fig.12. The current frequency of 50 kHz and measured time of 10 minutes were selected. The uncoated bioelectrode presented the largest impedance value and the amplitude of impedance was as high as 34 kΩ. It may be attributed that an insulating oxide layer was produced on the bioelectrode surface[47-48]. The existence of the oxide layer coating greatly increased the impedance value. Furthermore, the amplitude of impedance of bioelectrode with Ag layer and Ag–AgCl double layer was 2.4kΩ and 1.2kΩ, respectively. The lower impedance is desirable because the contact impedance will cause a potential drop and some attenuation of signal amplitude. As for stimulating electrode, the lower contact impedance could also reduce the energy consumption. Therefore, the bioelectrodes coated with Ag–AgCl double layer exhibited the lowest impedance value and was the best choice for the measurement of bioelectric signals.

4 Conclusion

In this study, the metal dry bioelectrodes with different coating layers were succesfully fabricated with laser micromilling and electroplating technology. When the Ag layer was coated on the bioelectrode surface, the Ag content increased with increasing electroplating time. However, the decrease of Ag layer weight was observed with much longer electroplating time, and the optimal electroplating time was 20 min. Later, the electrical impedance performance of bioelectrode coated with Ag layer and Ag–AgCl double layer was studied. The contact impedance between electrode and skin was measured using the two-electrode methods. Equivalent circuit of electrode-skin model was estabilished based on previous literatures. Compared

with the uncoated bioelectrode bioelectrode, the bioelectrode with Ag layer exhibits much lower impedance value and better impedance stability. Especially, when the bioelectrode is subsequently coated with Ag–AgCl double layer, the lowest impedance value and impedance stability are obtained. Thus, the metal dry bioelectrode coated with Ag–AgCl double layer have wide application prospect in bioelectric signal measurement.

Acknowledgments

This work was supported by the National Natural Science Foundation of China (Project No. 51475397), Science and technology Plan Project of Xiamen City (Project No. 3502Z20173024) and the Natural Science Fundation of Fujian Province of China (No. 2017J06015). In addition, the supports from the Open Fund of Beijing Advanced Innovation Center for Intelligent robots and systems (No.2016IRS21) are also acknowledged.

References

[1] P. S. Das, M.F. Hossain, J. Y. Park. Chemically reduced graphene oxide-based dry electrodes as touch sensor for electrocardiograph measurement. Microelectron. Eng. 180 (2017) 45-51.

[2] Y. Song, P. Li, M. Li, H. Li, C. Li, D. Sun, B. Yang. Fabrication of chitosan/Au-TiO_2 nanotube-based dry electrodes for electroencephalography recording. Mat. Sci. Eng. C-Mater. 79 (2017) 740-747.

[3] P.S. Das, J.Y. Park. A flexible touch sensor based on conductive elastomer for biopotential monitoring applications. Biomed. Signal. Proces. 33 (2017) 72-82.

[4] L. Jin, K.J. Kim, E.H. Song, Y.J. Ahn, Y.J. Jeong, T.I. Oh, E. J. Woo. Highly precise nanofiber web-based dry electrodes for vital signal monitoring. RSC Adv. 6 (2016) 40045-40057.

[5] N. Celik, N. Manivannan, A. Strudwick, W. Balachandran. Graphene-enabled electrodes for electrocardiogram monitoring. Nanomaterials 6 (2016) 156.

[6] H.L. Peng, J.Q. Liu, H.C. Tian, B. Xu, Y.Z. Dong, B. Yang, X. Chen, C.S. Yang. Flexible dry electrode based on carbon nanotube/polymer hybrid micropillars for biopotential recording. Sensor. Actuat. A 235 (2015) 48-56.

[7] L. Ren, Q. Jiang, K. Chen, Z. Chen, C. Pan, L. Jiang. Fabrication of a micro-needle array electrode by thermal drawing for bio-signals monitoring. Sensors 16 (2016) 908.

[8] G. Li, S. Wang, Y.Y. Duan. Towards gel-free electrodes: A systematic study of electrode-skin impedance. Sensor. Actuat. B 241 (2017) 1244-1255.

[9] K. Chen, L. Ren, Z. Chen, C. Pan, W. Zhou, L. Jiang. Fabrication of micro-needle electrodes for bio-signal recording by a magnetization-induced self-assembly method. Sensors 16(2016): 1533.

[10] N. Meziane, J.G. Webster, M. Attari, A.J. Nimunkar. Dry electrodes for electrocardiography. Physiol. Meas. 34 (2013) R47.

[11] A. Cömert, J. Hyttinen. Investigating the possible effect of electrode support structure on motion artifact in wearable bioelectric signal monitoring. Biomed. Eng.

Online 14 (2015) 44.

[12] A. Cömert, M. Honkala, J. Hyttinen. Effect of pressure and padding on motion artifact of textile electrodes. Biomed. Eng. Online 12 (2013) 26.

[13] C.T. Lin, L.D. Liao, Y.H. Liu, I.J. Wang, B.S. Lin, J.Y. Chang. Novel dry polymer foam electrodes for long-term EEG measurement. IEEE T. Bio-Med. Eng. 58 (2011) 1200-1207.

[14] T.I. Oh, S. Yoon, T.E. Kim, H. Wi, K.J. Kim, E.J. Woo, R.J. Sadleir. Nanofiber web textile dry electrodes for long-term biopotential recording. IEEE T. Biomed. Circ. S. 7 (2013) 204-211.

[15] S. Rajaraman, J.A. Bragg, J.D. Ross, M.G. Allen. Micromachined three-dimensional electrode arrays for transcutaneous nerve tracking. J. Micromech. MicroEng. 21 (2011) 085014.

[16] Y. Wang, W.H. Pei, K. Guo, Q. Gui, X.Q. Li, H.D. Chen, J.H. Yang. Dry electrode for the measurement of biopotential signals. Sci. China Inform. Sci. 54 (2011) 2435-2442.

[17] P. Griss, H.K. Tolvanen-Laakso, P. Merilainen, G. Stemme. Characterization of micromachined spiked biopotential electrodes. IEEE T. Bio-Med. Eng. 49 (2002) 597-604.

[18] P. Griss, P. Enoksson, H.K. Tolvanen-Laakso, P. Meriläinen, S. Ollmar, G. Stemme. Micromachined electrodes for biopotential measurements. J. Microelectromech. S. 10 (2001) 10-16.

[19] W.C. Ng, H.L. Seet, K.S. Lee, N. Ning, W.X. Tai, M. Sutedja, J.Y.H. Fuh, X.P. Li.

Micro-spike EEG electrode and the vacuum-casting technology for mass production. J. Mater. Process. Tech. 209 (2009) 4434-4438.

[20] P. Salvo, R. Raedt, E. Carrette, D. Schaubroeck, J. Vanfleteren, L. Cardon. A 3D printed dry electrode for ECG/EEG recording. Sensor. Actuat. A 174 (2012) 96-102.

[21] K. C. Chang, J. L. Kang, N. Y. Young, H. J. Eui, K. Woong, M. Byung-Kwon, R. WonHyoung. Spatially discrete thermal drawing of biodegradable microneedles for vascular drug delivery. Eur. J. Pharm. Biopharm. 83 (2013) 224–233.

[22] E.Z. Loizidou, N. T. Inoue, J. Ashton-Barnett, D.A. Barrow, C. J. Allender. Evaluation of geometrical effects of microneedles on skin penetration by CT scan and finite element analysis. Eur. J. Pharm. Biopharm. 107 (2016) 1–6.

[23]C.Pan, K.Chen, L. Jiang, Z. Chen, L. Ren, L. Liang, W. Yuan. Magnetization-induced self-assembly method: Micro-needle array fabrication. J. Mater. Process. Tech. 227 (2016) 251–258.

[24] F. Löffler. Functional metal-based coatings on ceramic substrates. Surf. Coat. Tech. 132 (2000) 222-227.

[25] F. Zhang, G.K. Wolf, X. Wang, X. Liu. Surface properties of silver doped titanium oxide films. Surf. Coat. Tech. 148 (2001) 65-70.

[26] Y. Guan, W. Zhou, H. Zheng, M.H. Hong, Y. Zhu, B.J. Qi. Effect of pulse duration on heat transfer and solidification development in laser-melt magnesium alloy. Appl. Phys. A 119 (2015) 437-442.

[27] Y.C. Guan, W. Zhou, Z.L. Li, H.Y. Zheng, G.C. Lim, M.H. Hong. Femtosecond laser-induced ripple structures on magnesium. Appl. Phys. A 115 (2014) 13-18.

[28] Z. Du, L. Chen, T.S. Kao, M.X. Wu, M.H. Hong. Improved optical limiting performance of laser-ablation-generated metal nanoparticles due to silica-microsphere-induced local field enhancement. Beilstein J. Nanotech. 6 (2015) 1199.

[29] R. Bomparola, S. Caporali, A. Lavacchi, U. Bardi. Silver electrodeposition from air and water-stable ionic liquid: An environmentally friendly alternative to cyanide baths. Surf. Coat. Tech. 201 (2007) 9485-9490.

[30] F. Ren, L. Yin, S. Wang, A.A. Volinsky, B. Tian. Cyanide-free silver electroplating process in thiosulfate bath and microstructure analysis of Ag coatings. T. Nonferr. Metal. Soc. 23 (2013) 3822-3828.

[31] B.J. Polk, A. Stelzenmuller, G. Mijares, W. MacCrehan, M. Gaitan. Ag/AgCl microelectrodes with improved stability for microfluidics. Sensor. Actuat. B 114 (2006) 239-247.

[32] W.D. Huang, H. Cao, S. Deb, M. Chiao, J.C. Chiao. A flexible pH sensor based on the iridium oxide sensing film. Sensor. Actuat. A 169 (2011) 1-11.

[33] J. Prado-Olivarez, F. Arellano-Olivares, A. Padilla-Medina, J. Diaz-Carmona, A. Ramirez-Agundis, A. Espinosa-Calderon, M. Garcia-Mesita, T. Aguilar-Diaz. Bioimpedance phase angle analysis of foot skin in diabetic patients: An experimental case study. IRBM, 36 (2015) 233-239.

[34] S. Xu, M. Dai, C. Xu, C.S. Chen, M.X. Tang, X.T. Shi, X.Z. Dong. Performance evaluation of five types of Ag/AgCl bio-electrodes for cerebral electrical impedance tomography. Ann. Biomed. Eng. 39 (2011) 2059-2067.

[35] W. Zhou, R. Song, X.L. Pan, Y.J. Peng, X.Y. Qi, J.H. Peng, K.S. Hui, K.N. Hui.

Fabrication and impedance measurement of novel metal dry bioelectrode . Sensor. Actuat. A 201 (2013) 127-133.

[36] W. Zhou, W.S. Lin, W. Liu, Y.J. Peng, J.H. Peng. Laser direct micromilling of copper-based bioelectrode with surface microstructure array. Opt. Laser. Eng. 73 (2015) 7-15.

[37] P. A. Jacquet. Adhesion of electrolytic copper deposits. Transactions of The Electrochemical Society 66 (1934) 393-426.

[38] Y. Pan, Y. Liu, T. Wang, X Lu. Effect of a Cu seed layer on electroplated Cu film. Microelectron. Eng. 105 (2013) 18-24.

[39] S. C. Kilchenmann, E. Rollo, E. Bianchi, C. Guiducci. Metal-coated silicon micropillars for freestanding 3D-electrode arrays in microchannels. Sensor. Actuat. B 185 (2013) 713-719.

[40] H.L. Peng, J.Q. Liu, H.C. Tian, Y.Z. Donge, B. Yang, X. Chen, C.S. Yang. A novel passive electrode based on porous Ti for EEG recording. Sensor. Actuat. B 226 (2016) 349-356.

[41] P. Fiedler, S. Griebel, P. Pedrosa, C. Fonseca, F. Vaz, L. Zentner, F. Zanow, J. Haueisen. Multichannel EEG with novel Ti/TiN dry electrodes. Sensor. Actuat. A 221 (2015) 139-147.

[42] S. Myllymaa, S. Pirinen, K. Myllymaa, M. Suvanto, T.A. Pakkanen, T.T. Pakkanen, R. Lappalainen. Improving electrochemical performance of flexible thin film electrodes with micropillar array structures. Meas. Sci. Technol. 23 (2012) 125701.

[43] E. T. McAdams, J. Jossinet, A. Lackermeier, F. Risacher. Factors affecting electrode-gel-skin interface impedance in electrical impedance tomography. Med. Biol. Eng. Comput. 34 (1996) 397-408.

[44] T. K. Bera, J. Nagaraju. Surface electrode switching of a 16-electrode wireless EIT system using RF-based digital data transmission scheme with 8 channel encoder/decoder ICs. Measurement 45 (2012) 541-555.

[45] M. Goharian, M. Soleimani, A. Jegatheesan, K. Chin, G.R. Moran. A DSP based multi-frequency 3D electrical impedance tomography system. Ann. Biomed. Eng. 36 (2008) 1594-1603.

[46] P. J. Langlois, Y. Wu, R.H. Bayford, A. Demosthenous. On the application of frequency selective common mode feedback for multifrequency EIT. Physiol. Meas. 36 (2015) 1337.

[47] C. Oruc, A. Altındal. Structural and dielectric properties of CuO nanoparticles. Ceram. Int. 43 (2017) 10708–10714.

[48] Y.J. Gan, Y. Wang, X. Dong, L. Dong. Microstructures and electrical properties of copper oxide doped terbium oxide ceramics. J. Mater. Sci.: Mater. Electron. 25 (2014) 4115–4121.

Authors Biography

Wei liu starts to work toward the Ph.D.degree in mechanical engineering at Xiamen University since 2014. Her research interests are in the area of design and measurement methods of different bioelectrodes.

Wei Zhou received received his Ph.D. degrees in mechanical engineering from South China University of Technology, Guangzhou, China,in 2010. From 2010 to 2012, he was a postdoc researcher at Sun Yat-sen University. He was appointed as an associate

professor in mechanical & electrical engineering of Xiamen University from Dec 2012 - Juy 2016. Now he is an professor at Xiamen University. His current research interests
focus on design, fabrication and performance evaluation of biomedical device.

Shaoyu Liu starts to work toward the Ph.D. degree in mechanical engineering at Xiamen University 2014. His research interests are in microfabrication technology of biomedical device.

Chenying Zhang starts to work toward the Ph.D. degree in mechanical engineering at Xiamen University since 2014. His research interests are in the area of the optimization of fabrication process of bioelectrodes.

Shuaishuai Huang starts to work toward the M.D. degree in mechanical engineering at Xiamen University since 2015. Her research interests are in the area of microfabrication
methods of bioelectrode.

Yaoyao Li starts to work toward the M.D. degree in mechanical engineering at Xiamen University since 2017. Her research interests are in the area of modeling and simulation
of microfabrication process of bioelectrode.

Kwan San Hui received his PhD degree in the department of mechanical engineering at the Hong Kong University of Science and Technology in 2008. He was appointed as a lecturer in department of systems engineering and engineering management of City University of Hong Kong, Hong Kong from Aug 2008 - Feb 2012. In Mar 2013, he worked as an Assistant Professor in Department of Mechanical Engineering at Hanyang University, South Korea. In Sep 2016, he was appointed as a Lecturer in Mechanical Engineering, School of Mathematics, Faculty of Science, University of East Anglia, UK. He has extensive research experience in material science, catalysis, air/water pollution
control, and energy storage.

Figure captions

Fig.1 Structural design of metal dry bioelectrode: 1-Back side of bioelectrode; 2-Front side of bioelectrode; 3-Shielding wire; 4-Conductive silver glue; 5-Metal electrode core with surface microstructures arrays; 6-Foam backing material

Fig.2 Schematic of fabrication method of metal electrode core using laser

micromilling technology

Fig.3 The illustration of the electroplating process of bioelectrode coated with Ag and Ag–AgCl double layer: 1- Cathode; 2- Anode; 3-Solution

Fig.4 SEM images of surface microstructure array of dry bioelectrode

Fig.5 Characterization of eletroplated coating of dry bioelectrode: (a)Ag concentration with different electroplating time;(b) X-ray photoelectron spectroscopy;

Fig.6 Measured impedance of bioelectrode with different electroplating times

Fig.7 Concentration of silver and chloride element of biolectrode when the Ag–AgCl double layer was deposited

Fig.8 Equivalent circuit model for electrode-skin interface

Fig.9 Bode plots of the measured impedance of bioelectrodes coated with Ag and Ag–AgCl double layer: (a) Amplitude ; (b)Phase

Fig.10 Nyquist plots of the measured impedance of bioelectrodes with different surface coatings: (a) Ag layer; (b) Ag–AgCl double layer

Fig.11 Impedance stability of two bioelectrodes coated with Ag layer and Ag–AgCl double layer

Fig.12 Measured impedances of bioelectrodes with different surface coatings

Table 1 Specifications of characteristic parameters of the used fiber laser system

Characteristic	Parameter range	Process conditions	Unit
Wavelength	1055 - 1070	1064	nm
Pulse duration	90 - 120	100	ns
Repetition rate	20 - 200	20	kHz
Focused diameter	24.3 – 37.3	31.5	μm

Laser output power	0 - 30	20	W

Table 2 Characteristic parameters of electroplating solution systems

Parameter	Concentration（g/L）	Production manufacturer
$AgNO_3$	40	Xilong Chemical Co., Ltd, China
$Na_2S_2O_3$	225	Xilong Chemical Co., Ltd, China
$K_2S_2O_5$	40	Xilong Chemical Co., Ltd, China
CH_3COONH_4	25	Xilong Chemical Co., Ltd, China
CH_5N_3S	0.8	Pharmaceutical Group Chemical Reagent Co., Ltd, China

Table 3 Numerical fitting results of equivalent circuit components of two bioelectrodes coated with Ag layer and Ag–AgCl double layer

	Rs (Ω)	CPE-T (F)	CPE-P	Rct (Ω)
Bioelectrode coated with Ag/AgCl double layer	207	6.34×10^{-8}	0.811	4.26×10^{4}
Bioelectrode coated with Ag layer	238	4.63×10^{-8}	0.719	2.45×10^{6}

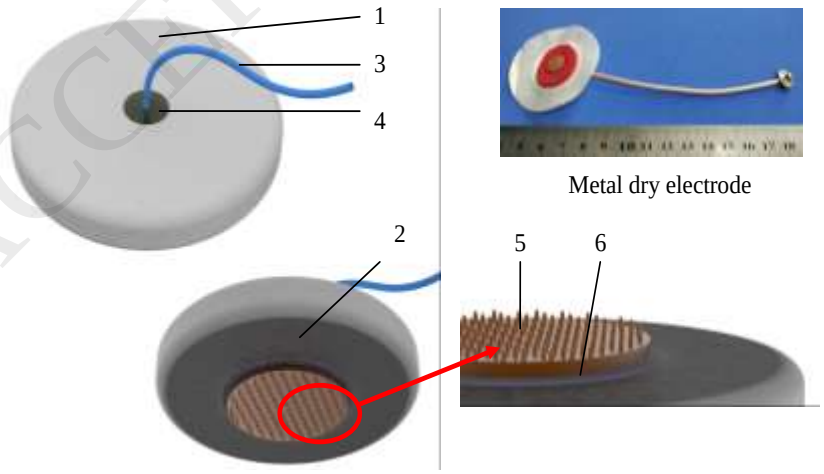

Fig.1

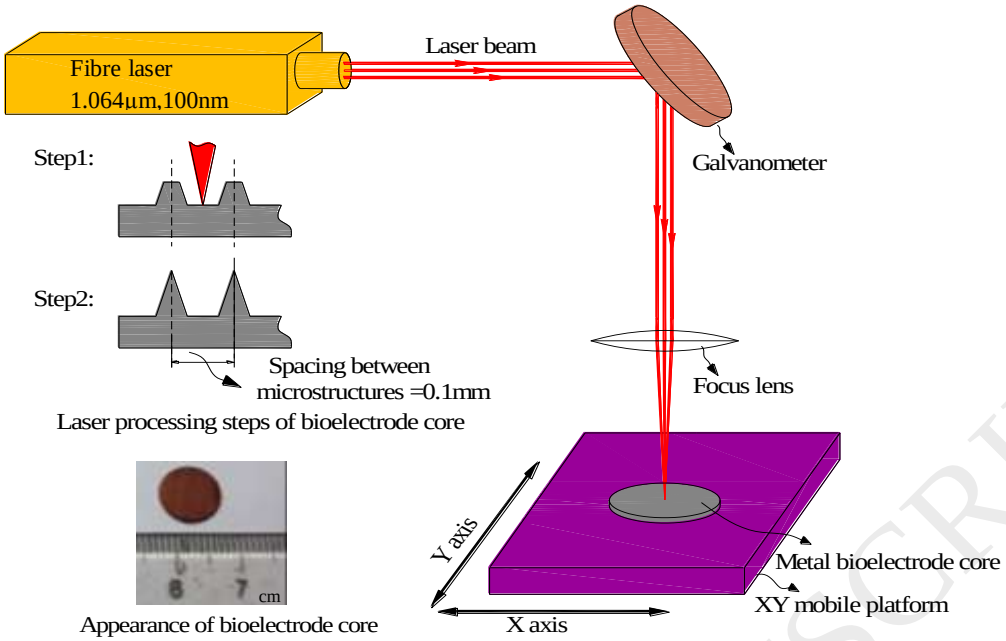

Fig.2

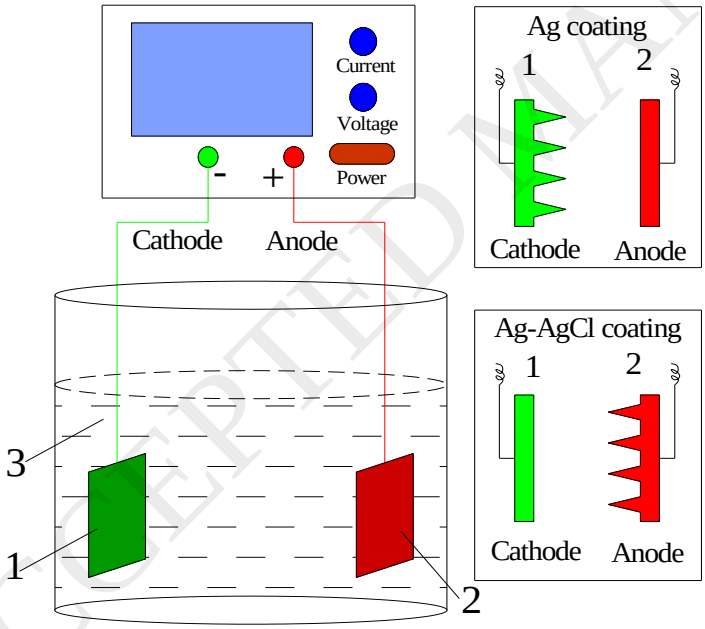

Fig.3

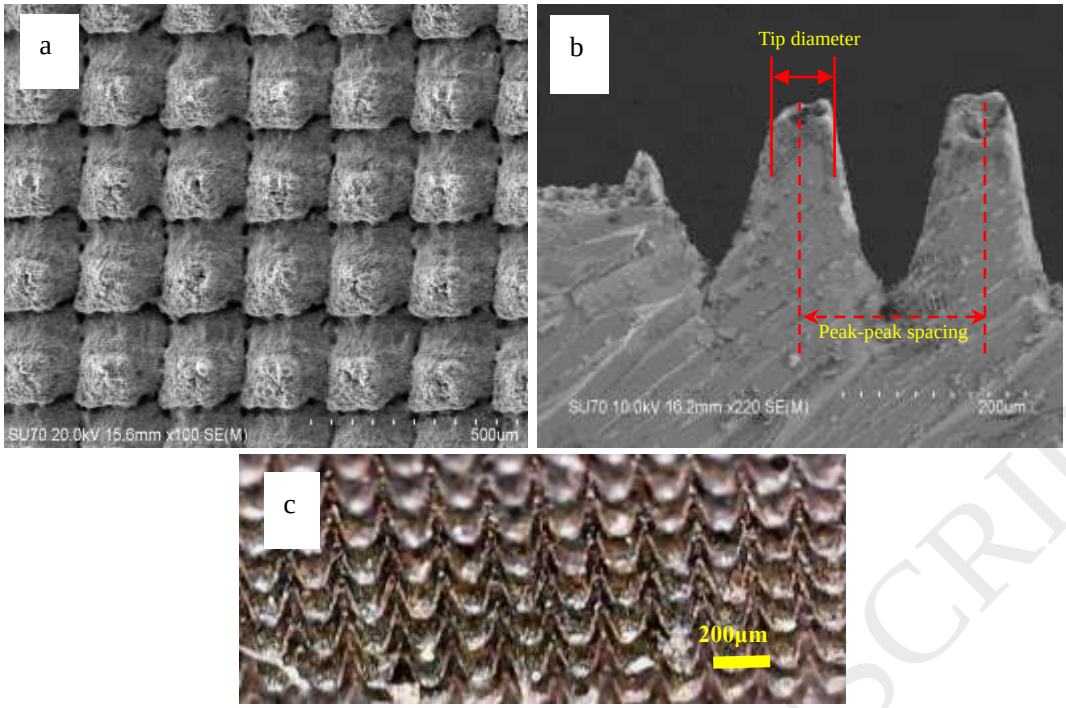

Fig.4

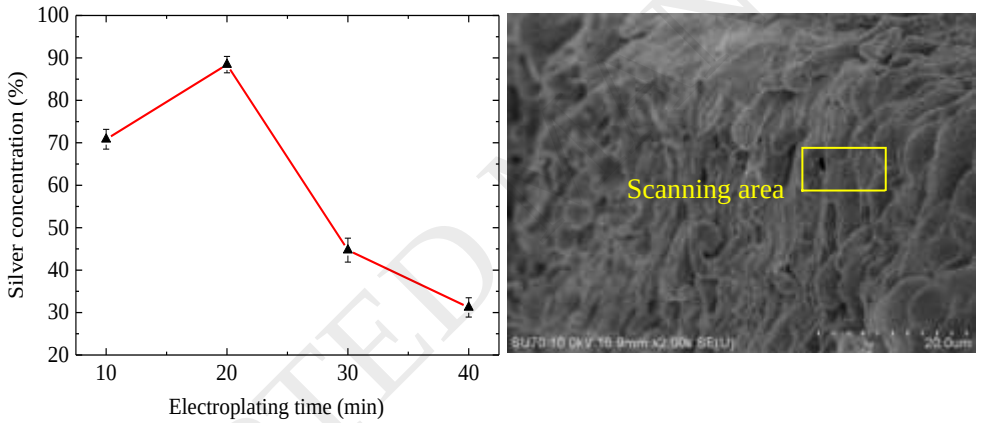

(a)

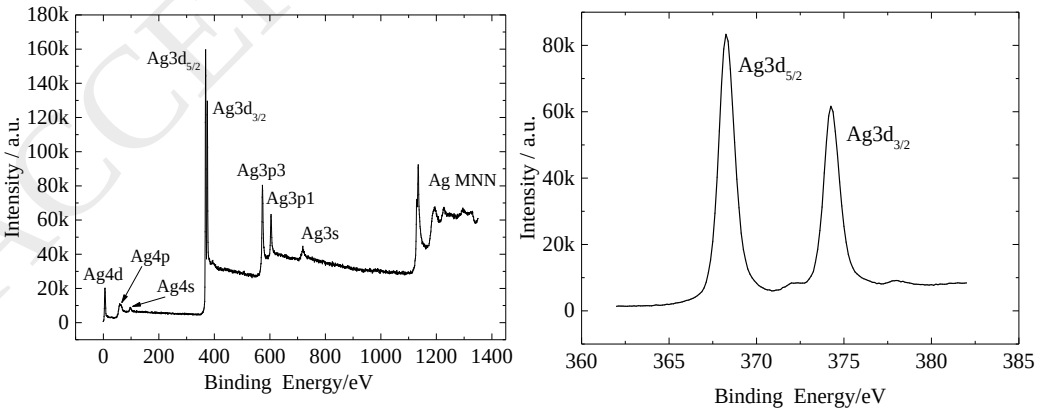

(b)

Fig.5

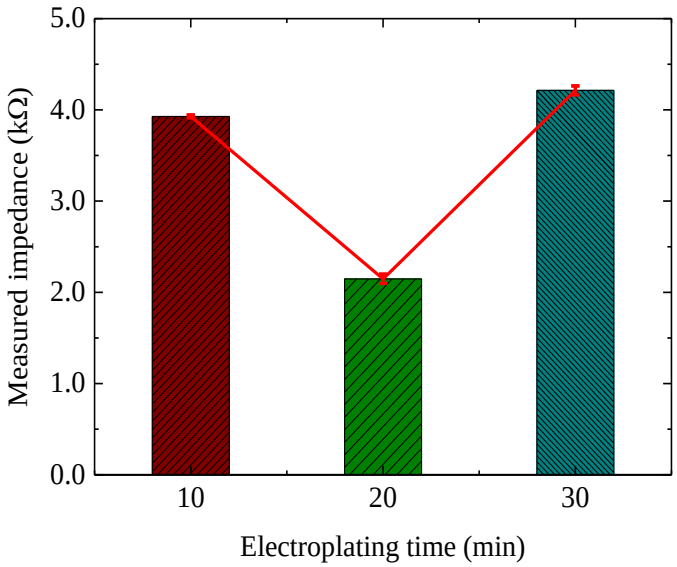

Fig.6

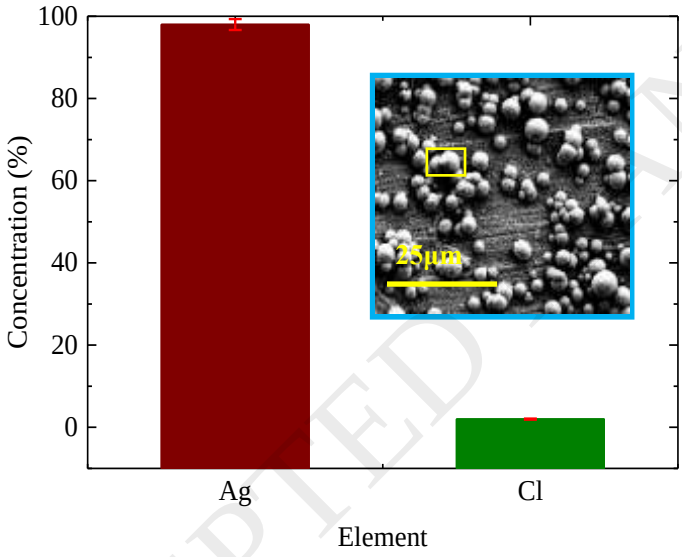

Fig.7

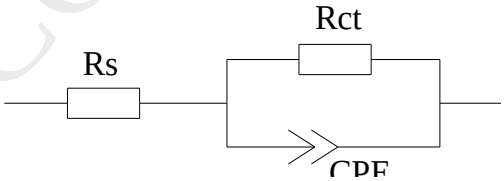

Fig.8

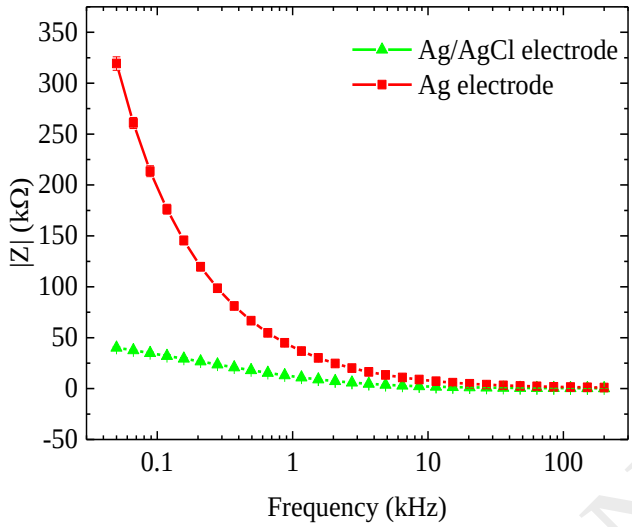

(a)

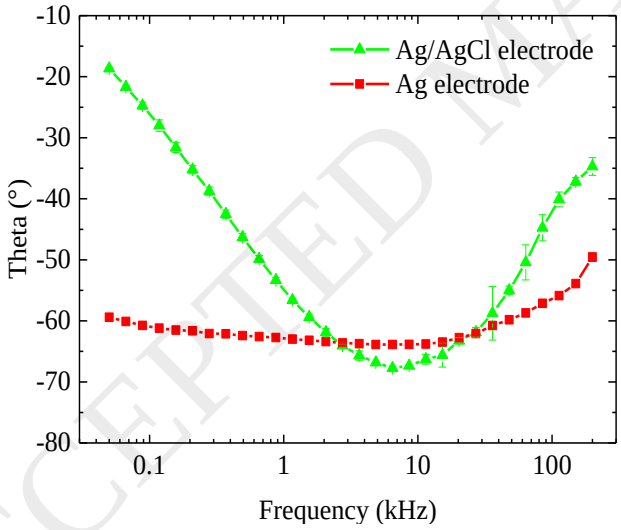

(b)

Fig.9

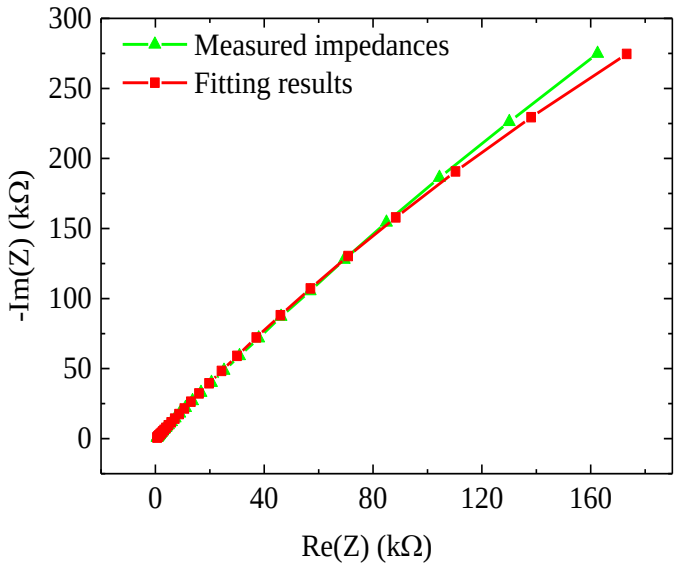

(a)

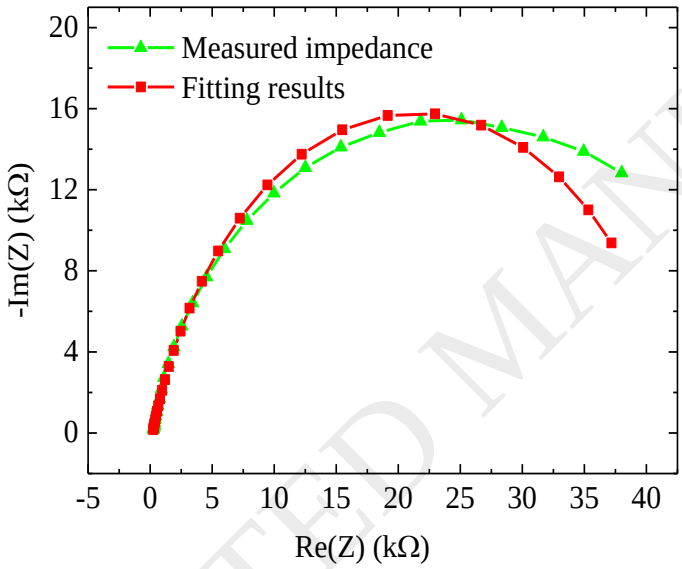

(b)

Fig.10

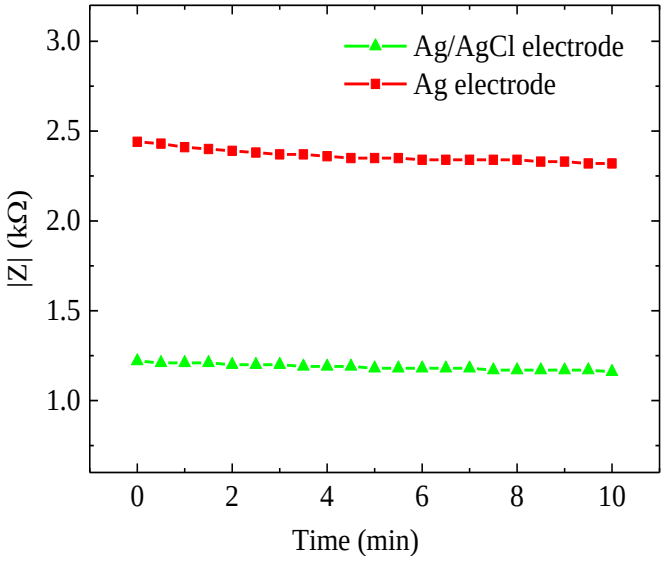

Fig.11

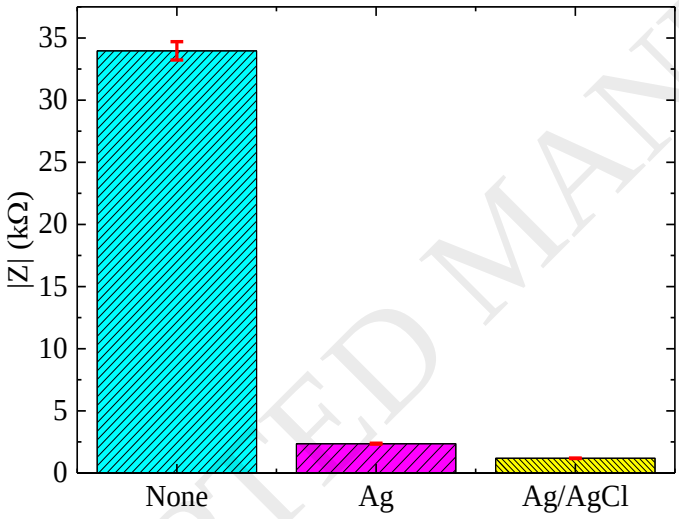

Fig.12